CCC Publications

AGORA
UNIVERSITY PRESS

Optimized CNN-based Brain Tumor Segmentation and Classification using Artificial Bee Colony and Thresholding

P. Ashok Babu, B.V. Subba Rao, Y. Vijay Bhaskar Reddy,
G .Rajendra Kumar, J. Nageswara Rao, Surendra Kumar Reddy Koduru, G Sunil Kumar

P. Ashok Babu

Department of Electronics and Communication Engineering,
Institute of Aeronautical Enginnering, Hyderbad, India
Corresponding author: ashokbabup2@gmail.com

B.V. Subba Rao

Department of Information Technology
PVP Siddhartha Institute of Technology,Andhra Pradesh, India
bvsrau@gmail.com

Y. Vijay Bhaskar Reddy

Department of Computer Science and Engineering,
Lakireddy Bali Reddy College of Engineering, Mylavaram, NTR District, PIN-521230, Andhra Pradesh, India,
yaramala.vijay@gmail.com

G. Rajendra Kumar

Department of IT, Vignan's Institute of Information Technology, Visakhapatnam – 530049, A.P, India.
rajendragk@rediffmail.com

J. Nageswara Rao

Department of Computer Science and Engineering,
Lakireddy Bali Reddy College of Engineering, Mylavaram, NTR District, PIN-521230, Andhra Pradesh, India,
nagsmit@gmail.com

Surendra Kumar Reddy Koduru

Business Intelligence and Reporting Lead, NC, USA
surendrakoduru.bi@gmail.com

G. Sunil Kumar

Department of ECE,
CMR College of Engineering & Technology, Hyderabad, India.
gsunilmtech@gmail.com

Abstract

One of the most important tasks used by the medical profession for disease identification and recovery preparation is automatic medical image processing. Statistical approaches are the most commonly used algorithms, and they consist several important step. Brain tumors are the foremost causes of death of cancerous diseases all over the world. The hippocampus is the human body's primary control structure. Since a tumor attacks the brain, it can kill the patient if it is not detected early. Among the various imaging modalities available, Magnetic Resonance Image (MRI) is a better implement for calculating area and classifying tumors based on their grade. MRI does not emit any toxic radiation. There is currently no automated method for detecting and identifying the grade of a tumor. This study mainly focusses on classifying and segmenting brain tumors from MRI scan data. It aids physicians in the planning of future care or surgery. This procedure consists of four steps: image de-noising, tumor extraction, attribute extraction, and hybrid classification. In the first step of image de-noising, the curvelet transformation (CT) is used. Then, in the next stage, Artificial Bee Colony (ABC) Optimization is used in conjunction with the thresholding process to remove tumors from brain MRI scans. Another optimization approach is used to recover the learning rate of the Convolutional Neural Network for the final hybrid classification. The experiment model is assessed by using the multimodal brain tumor (BRATS) 2013 and 2015 challenge datasets from medical image computing. The outcomes of the experiment presented that the method achieved the segmentation 95.23% and 94% of accuracy, where the proposed optimized CNN achieved classification accuracy of 98.5% and 99% for both datasets.

Keywords: Artificial Bee Colony; Brain tumor; Magnetic Resonance Image; Medical Image Analysis; Thresholding method;

1 Introduction

Brain tumor is a group of rare or unusual cells found inner part of the brain. The skull is the brain's rigid exterior coating that acts as a shield in the event of an injury. Any irregular cell growth inside it will pose a serious problem [1-2]. There are two kinds of brain tumors: malignant, which is more severe and harder to treat, and benign, which is curable if diagnosed early [3]. Furthermore, primary and metastatic are the brain tumors, The predominant type brain tumors that ascend from glial cells are called Gliomas, and about 70% of adults have this form of cancer. Two classification ratings that tumor cells proliferate are: low grade (oligodendroglia) and (glioblastoma) high grade [4]. If tumor is noticed at an initial stage, they are fewer harmful than when they are discovered later in the disease's progression, which reduces patient lifespan to less than two years. The most effective cure for tumor patients is chemotherapy, radiation, surgery, or a combination of these. Figure 1 depicts a brain representation of a malignant tumor, a healthy brain, and a benign tumor.
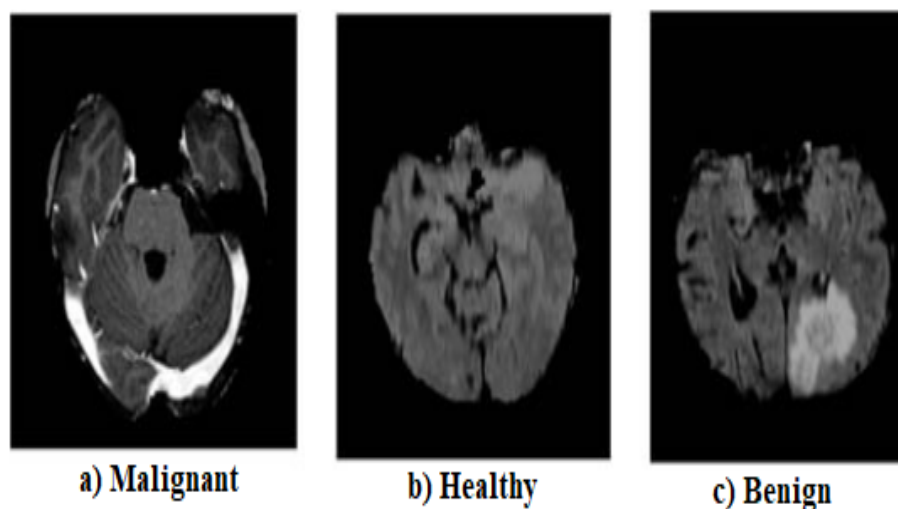

a) Malignant   b) Healthy   c) Benign

Figure 1: Sample MRI images of Brain

MRI is the most commonly used imaging technology tool that play an important role in identifying brain tumors [5]. MRI is a non-invasive model with enhanced contrast of soft tissues that provides information about

tumor site, shape, and scale in the non-appearance of high ionization radiations [6]. Figure 2 depicts the reference scans.
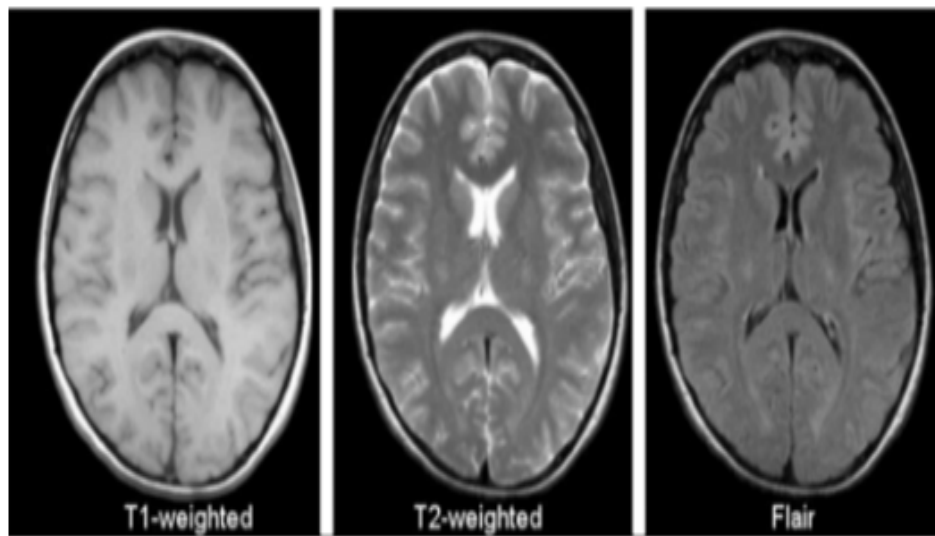

Figure 2: Sample MRI Images

The MR images segmentation process [7] is a critical role in monitoring tumor volume variance. It is critical in radiotherapy and surgical preparation where affected and stable areas are specifically separated [8-9]. Currently, manual segmentation is more prevalent in clinical routines where radiologists must put in more clinical experience and effort. Manual diagnosis and segmentation of brain tumors does not yield reliable results and is a time-consuming and inefficient procedure [10]. Furthermore, tumor form, diameter, texture, scale, position, and abnormality are all typical issues in current systems. Automatic approaches to detecting brain tumors are more notable and meaningful. Brain tumor segmentation using 2D MRI slices are classified into major following types: threshold and region-based [11-15], pixel-based scheme [16-18]. Threshold methods do not have a single threshold for classifying target voxel segmentation based on intensities. To outline the edges of voxels, the Sobel filter is used. Then, to optimize the performance, the pixel of every voxel are associated to threshold parameters, and each pixel is allocated to neighboring regions. In healthcare imaging, the automatic detection of risky human illnesses such as tumors in brain, stomach infections, skin cancer, and lung cancer are very common illnesses. For the detection of these diseases, multiple segmentation and classification approaches focused on computer vision (CV) available [19]. Brain tumors are the most important and risky form of cancer in medical imaging, and numerous computerized approaches for diagnosing them have recently been developed. Established procedures generally require several stages like noise isolation pre-processing, segmentation of tumor region, useful feature extraction, redundant feature reduction, and categorization. Ariyo et al. [20] the Spatial Fuzzy C-Means plus K-means Algorithm was proposed, a strategy for distinguishing dysfunctional brain tissues from stable brain tissues. The noise is reduced in this technique by merging the spatial equation to the FCM algorithm, and the optimum likelihood for pixels with particular membership is achieved by using the K-means algorithm. Sharif et al. [21] have identified a multi-features selection for brain tumor segmentation using enhanced binomial thresholding. For segmentation, a Gaussian filter for pre-processing, and an enhanced thresholding system with certain morphological operations is used. Following that, a serial-based approach for fusing derived geometric and Harlick features is introduced. Finally, best features are selected from the fused vector using GA, and classification is done using LSVM. Damodharan et al. [22] brain tumor revealing scheme based on the combination of segmentation and neural networks was proposed. The applied approach's success is evaluated by comparing its findings to those of other classification methods such as NN, KNN, and Bayesian classification in terms of precision, specificity, and sensitivity. Pereira et al. [23] used MRI images to apply an approach focused on Convolution Neural Networks (CNN) for effective tumor extraction. To isolate and identify the tumor region from brain MRI scans, Bahadure et al. [24] used a classification system focused on Bayesian fuzzy clustering. As compared to a few previously applied methods, the presented process performs well in terms of precision. Sharma et al. [25] developed a hybrid method for reliably extracting tumor regions as well as classifying brain tumors. This presented methodology includes three primary steps: pre-processing- thresholding, morphological procedures, and watershed segmentation; and post-processing- watershed segmentation. Segmented MRI scans are used to remove GLCM characteristics, and the tumor is classified using the KMNN classifier. To derive details from CNN architecture such as UNet [26] and DeepMedic [27], the Hyper column paradigm is used [28]. Furthermore, U-net and its updated systems are

S.NO.	AUTHOR	METHOD	LIMITATION
1.	Md. Sujan et.al 2016	A novel method for locating a brain tumour that combines thresholding and morphological image analysis.	For large datasets, this technique is not suitable.
2.	D. Ravi et.al 2017	A novel method for tumour classification mapping that reduces dimensionality	The detection rate is reduced on based on sample quantity.
3.	A. Raju et.al 2018	HCS optimization techniques based on SVNN classifier were used to classify brain tumours using the Bayesian Fuzzy Clustering (BFC) methodology.	Lack of pre-processing step and less efficient.
4.	K. Usman et.al 2017	A Multi-modality MRI brain tumour segmentation and classification scheme	Poor robustness for large datasets
5.	M. Soltaninejad et.al 2017	An approach that employs Super Pixel-based Extremely Randomness Trees (SPERTs) to automatically identify and segment brain tumours.	Less accurate.

an important collection of architecture for segmenting medical images [29]. The model of down/up-sampling operations. By doing successive concatenation, the U-net architecture shows function planning in the model of encoding to decoding [30]. Several approaches are discussed in the literature, but none of them produce better outcomes in all efficiency indicators. On five challenging datasets, the model proposed performed well across the board in terms of all output metrics. This thesis looks at a new score level fusion technique for reliably segmenting and detecting brain tumors using MRI.

The threshold selection criteria used in this study is the ABC optimization algorithm. The algorithm is used in conjunction with the thresholding process to extract tumors from brain MRI scans. The thresholding process is used in tumor region seperation from the rest of the image by identifying the intensity level at which the tumor is distinguishable from the surrounding tissue. The ABC algorithm is used to optimize the threshold value by adjusting it until the best segmentation of the tumor is achieved. The goal of the algorithm is to reduce the discrepancy between the identified tumor location in the image (segmented tumor) and its actual location (ground truth). The algorithm is run multiple times with different initial threshold values and the final value of threshold is selected based on the one that gives the best segmentation results. This process allows for a more accurate and efficient extraction of the tumor from the MRI scan.

1.1 Problem Statement

Our primary emphasis in this effort is on the accurate brain tumors segmentation and subsequent classification into related groups. Several difficulties exist for this procedure, including small contrast tumor, size, diameter, unrelated characteristics, and a few others. Whereas in this work, we concentrate on tumor improvement and the removal of irrelevant characteristics for the highest segmentation and classification precision.

1.2 Major contributions

The major influence of our method is described as follows.

The CT is used to improve the appearance of the originality tumor from a certain angle and scale. The segmentation of tumor is accomplished using ABC in conjunction with the thresholding process. Form and texture are two examples of multi-type features extracted. Then, for trivial feature reduction, a modern technique known as Berkeley Wavelet Transformation is used. A novel approach to classifying tumor/non-tumor MR images is proposed during the classification process, a pre-train CNN ideal and the segmented images are fed in it, then feature learning is conducted using Alex net. For the relevance of this methodology, it is compared to other classification approaches and current techniques.

The chief objectives are:

1. To develop a new strategy for automatic detection and segmentation from MRI data of brain images.

2. To effectively validate of method proposed by accurately segmenting and classifying brain tumors as benign or malignant.

3. To optimize the learning rate of a CNN for better classification performance.

4. Validation by using the multimodal brain tumor (BRATS) 2013 and 2015 challenge datasets.

5. To explore the potential for further development of the method for segmenting and identifying sub-tumoral parts, and for integration with multiple classifiers to improve precision and diagnostic confidence index (DCI).

Organization of this paper is arranged as follows: The brief explanation of proposed methodology along with flow chart is presented in Section 2. The validation of projected segmentation and classification techniques with existing techniques are given in Section 3. The conclusion and future enhancement is described in Section 4.

2 Proposed Methodology

A five step method of proposed work that are primarily the input image is pre-processing, tumor segmentation using ABC and thresholding, extraction of a small number of beneficial features, superlative features collection constructed with high importance, and feature fusion. Later, these attributes are fed into a CNN classifier to be included in the classification procedure. Figure 3 depicts a flow diagram of the proposed solution. The proposed method for classifying and segmenting brain tumors from MRI data consists of four main steps:

1. Image de-noising: In this step, the curvelet transformation (CT) removes noise from the brain MRI scans. This step is necessary to improve the accuracy of the subsequent steps.

2. Tumor extraction: Artificial Bee Colony (ABC) Optimization is used in conjunction with the thresholding process for extraction of brain tumor from the denoised images. ABC optimization is employed to identify the optimal value of threshold that separates the tumor from the healthy tissue.

3. Attribute extraction: In this step, the extracted tumor is passed through the Berkeley Wavelet Transformation (BWT) for feature extraction. BWT is used to extract features such as the size, shape, and texture of the tumor that are used for classification.

4. Hybrid classification: The feature extraction from aforementioned process serves as for classification input to CNN. The rate of learning the CNN is optimized using the Butterfly optimization algorithm for better classification accuracy. The CNN is trained using the BRATS 2013 and 2015 datasets to categorize the tumors as malignant or benign.

2.1 CT for Image Enhancement

CT is used to reduce excess noise in an input image by improving the tumor region. This approach is advantageous in terms of execution ease, illness reliability, and turnaround time. Also, the CT achieves optimum recovery of corners, as well as dim linear and curve functions. In terms of image de-noising efficiency, the use of ridgelet transforms, i.e. CT, is more effective than the use of wavelet transform. The ridgelet transform is transformed into the Radon transform. To apply a support interval or to scale in the ridgelet transform, an anisotropy scaling relationship is used. A multi-scaling ridgelet is used to decompose the curve or edge into blocks and sub-blocks. Furthermore, for the purposes of ridgelet analysis implementation, these sub-blocks are loosely regarded as straight lines. In equation, the decomposition stages of the CT are mathematically defined as follows (1).
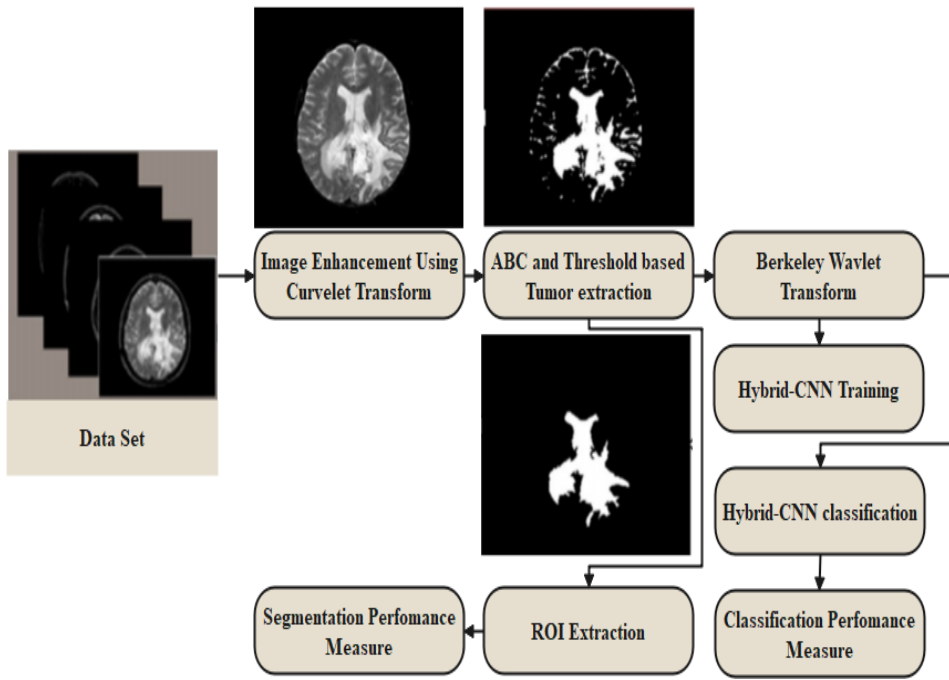
Figure 3: Working Flow of proposed methodology

$$g\text{ß}(F_0 g, \Delta_1 g, \ \Delta_2 g, \ \dots,) \tag{1}$$

Where, F_0 signifies filters of sub-bands, Δ_b signifies sub-bands data 2^{-2b} and g signified a tumor particle. The $k_1 \ and \ k_2$ are image set size. The mathematical relative is clarified in equation (2).

$$Q = \left[\frac{K_1}{2^b}, \frac{(K_1+1)}{2^b}\right] \times \left[\frac{K_2}{2^b}, \frac{(K_2+1)}{2^b}\right] \tag{2}$$

Following that, the resulting square to unit size is renormalized. This step's quantitative relationship is expressed mathematically as follows:

$$h_Q = F^{-1} Q\left(V_Q \Delta_b g\right), \ Q \in Q_b$$

Where, $(F_Q g)(x_1, x_2) = 2^b g(2^b x_1 - K_1, \ 2^b x_2 - K_2)$ and proves the renormalization operative model. Here, two dyadic sub-bands $\left[2^{2b}, 2^{2b+1}\right] \ and \ \left[2^{2b+1}, 2^{2b+2}\right]$ are integrated before implementing the ridgelet transform.

$$\propto_\mu = \langle h_Q, \ p\lambda \rangle \tag{3}$$

The denoising results after put on the CT are signified in Figure 4.

2.2 ABC and thresholding based tumor extraction

ABC has the capabilities of fully showing the space of the feasible solution and being insensitive to noise. The traditional ABC separates bees into three categories namely, employed, onlooker and scout bees. They have different jobs. Employed bees randomly search for honey and share information together. Onlooker bees learn from employed bees, and then take over their jobs. Scout bee is a supervisor, if it discovers some onlooker bees are unable to find the honey in limited time, it will send an employed bee to replace one of them. In this developed ABC, Cauchy perturbation strategy is applied to overcome the disadvantage of being easy to drop into the local optimum. The detailed description of ABC is as follows.

1. **Parameter Setting and Population Initialization**

$$X = rand\left(NP, D\right) * (ub - lb) + ones\left(NP, D\right) * lb \tag{4}$$
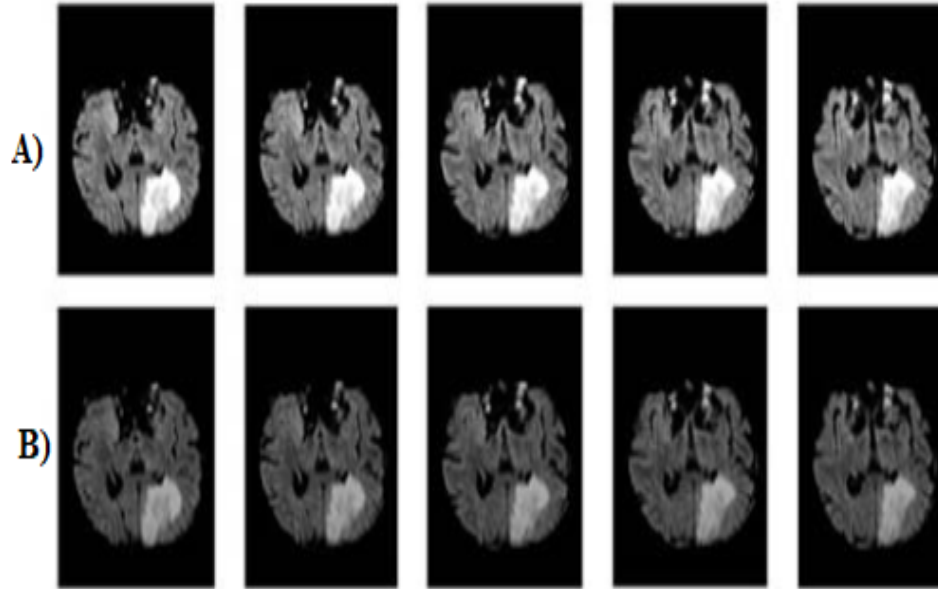
$$V = rand\left(NP, D\right) \tag{5}$$

Figure 4: Sample de-noised MRI images using CT. A) Original Images B)

1. **Employed Bee Phase and the Map and Compass Operator**

This process unites two traditional operations. First of all, the ith individual generates a random number S in$(0, 1)$. Then it compares with 0.5, if S is greater than 0.5 , this process executes the improved employed bee phase, otherwise it executes the traditional map and compass operator.

Eqs (6) and (??) show that ith and the kth individuals share the jth dimension information. In this paper, multiple dimensions are selected randomly in $(1, D)$. The factor $p(i)$ affects the degree of information communication by value of parameter$trail(i)$. When $trail(i)$ is small, it means that the ith individual has won in a short time, which should retain more of their nature. The range of $p(i)$ is $\left(\frac{4}{\pi} * \arctan\left(\frac{1}{D}\right), 1\right)$. Eqs (5) reflects the positive relationship between $trail(i)$ and$P(i)$. The former represents the speed of the ith individual approaching the optimum, where iteration is the current iteration, rand is a randomly in $(0, 1)$, and $X_b$is the best position of the whole population. The latter indicates the ith individual's new position after moving at a new speed. New population updates according to Eqs. (??)–(10), and then they are brought into Eqs. (4)–(6) respectively to calculate energy values. In order to make greedy selection, the fitness of each energy value is calculated by Eq. (??). In this paper, the lower the energy value is, the greater the fitness preforms. When the energy value is positive, the fitness is less than 1. And when the energy value is negative, the fitness is greater than 1.

$$p(i) = \frac{4}{\pi}\arctan(\frac{trail(i)}{D}) \tag{6}$$

$$X_i^j \, X_i^j + rand * \left(X_i^j - X_i^j\right) * p(i)$$

$$V_i = V_i * e^{-iter} + rand * (X_b - X_i,), \; i \in \{1, 2, \ldots NP\} \tag{7}$$

$$X_i = X_i + V_i, \;\; i \in \{1, 2, \ldots.NP\} \tag{8}$$

1. **Onlooker Bee Phase**

Equation (??) shows the ith and kth individuals share the jth dimension information. What's different from traditional phase is roulette selection. The idea of roulette selection is to allow individuals with high fitness to breed while individuals with low fitness to have no or less opportunities to reproduce. In order for all individuals to communicate, the roulette selection should be deleted.

$$X_i^j \, X_i^j + rand \; (X_k^j \, X_i^j)$$

1. **The Landmark Operator**

Equation (9) calculates the central position by weight of population's fitness. In the traditional ABC, X_c is obtained by all the reserved individuals, and the population is halved through every iteration. This paper keeps the number of populations. At the same time, it performs the following steps: firstly, all individuals rank according to their fitness from high to low. Then, select the front $1/3$ of population to calculate X_c. Finally update the behind $1/3$ of population according to Equation (10).

In Eq. (10), *iter* is the recent iteration, cycle is the total iterations. The range of $u(i)$ is $(0.1, 1)$. As the increases of *iter*, the population gets father and father away X_c so, the extent of convergence is alleviated.

$$X_c = \frac{\sum_{i=1}^{NP} X_i * fitness(i)}{NP * \sum_{i=1}^{NP} fitness(i)} \tag{9}$$

$$u(i) = exp - \left\{ \left(\frac{iter - 1}{cycle - 1} \right) * in\ (10) \right\} \tag{10}$$

$$X_i = X_i + rand * (X_{center} - X_i) * u(i) \tag{11}$$

1. **Scout Bee Phase**

When $trial(i)$ reaches the upper $limit D$, it means that the ith individual has not updated its position in D times and falls into local optima. To increase the diversity of population, when $trial(i) > D$, the ith individual requires to reinitialize by Eq. (**??**).

$$X_i = rand\,(1, D) * (ub\ -\ lb) + ones\,(1, D) * lb \tag{12}$$

1. **Cauchy Perturbation**

In order to move out of the local optimal solution, Cauchy perturbation strategy is introduced. The Cauchy probability density function is as shown in Eq. (**??**), where x_0 controls the position of X axis and γ controls the size of Y axis. According to this work, $x_0 = 0$, $\gamma = 1$. The distribution function of Cauchy perturbation is Eq. (13) which is obtained by Eq. (**??**) and the above parameters. $c(1, D)$ Means a vector consisting of D random numbers which generate by Eq. (14). In Eq. (15), X_b is the best individual.

$$f(x; x_0, \gamma) = \frac{1}{\pi} \left[\frac{\gamma}{(x - x_0)^2 + \gamma^2} \right] \tag{13}$$

$$c(x) = \frac{1}{2} + \frac{1}{\pi} \arctan(x) \tag{14}$$

$$X_b = X_b + c(1, D) * (ub - lb) \tag{15}$$

The procedure of final decision
To decide the end of the algorithm, a predetermined number of rounds are used; each of these loops is made up of fixed steps. Finally, a binary determination is made at each pixel location to determine if it was existent on the outside boundary or not. This is accomplished by applying a threshold value T to the final resultant. Cauchy Perturbation is an abbreviation for Cauchy Perturbation

2.3   Feature Extraction using Berkeley Wavelet Transformation

BWT is used for efficient segmentation of brain MR images. In reality, it is the first research of its kind to utilize Berkeley wavelet transformation for brain MR image segmentation. The Berkeley wavelet transformation method is underlined in order to break down data functions into components of varying frequencies, allowing each component to be studied separately. Since it is the other wavelets source and is distinct by Eq. 19, from a simple wavelet $\Psi(t)$ all wavelets are formed. Where, s and τ are the translation factors, correspondingly. The wavelet creates a whole, orthonormal basis in 2-D by scaling and translating the it with a single wavelet constant term. β_x^φ is a piecewise constant function of the mother wavelet transformation. Eq. 20 shows how wavelets are substituted from the mother wavelet β_x^φ are generated at different pixel positions.

$$\beta_x^\varphi(\tau, s) = \frac{1}{s^2} \beta_x^\varphi (3^s\,(x - i), 3^s(y - j)) \tag{16}$$

Where x and s are the wavelet transformation's translation and scale parameters, respectively, and β_x^φ is the function for transforming, and this is known as the BWT mother wavelet.

2.4   Hybrid Classification

In this section, a quick explanation of hybrid classification that uses Butterfly optimization for CNN learning rate optimization is given. The CNN is first described as follows:

2.4.1 Convolutional Neural Network

For training, CNN utilizes a backpropagation algorithm [31] and trained samples for inputs vector X to the CNN's target class y function. The desired goal is learnt by comparing with each CNN's output and the modification among them generates an error of learning, the next-generation CNN role is assumed and is given by,

$$E\left(\omega\right) = \frac{1}{2}\sum_{\rho=1}^{p}\sum_{j=1}^{N_\iota}\left(o_{j,p}^{l} - y_{j,p}\right)^2 \tag{17}$$

This minimising of cost function $E\left(\omega\right),$
discovery a minimizer $\widetilde{\omega} = \widetilde{\omega}^1, \widetilde{\omega}^2, \ldots, \widetilde{\omega}^v \epsilon \mathbb{R}^v,$ where $\mathrm{v} = \sum_{k=1}^{L} \mathrm{WeightNum}\ (\mathrm{k}).$

$$\omega_{i+1} = \omega_i - n\nabla E_i\left(\omega_i\right) \tag{18}$$

Where n is the value of learning rate. The n is designated by BOA method.

2.4.2 Butterfly Optimization Algorithm (BOA)

Butterflies are BOA's search agents that optimize results. A butterfly can emit fragrance of differing intensity depending on its health, i.e., when a butterfly travels from one place to another, its fitness will change consequently. The scent will disperse through time and space, and other butterflies will be able to sense it, encouraging butterflies to exchange personal information and form a common social awareness network. The suggested method refers to this behavior as global quest, which occurs on one butterfly identifying the smell of one more butterfly. Scent-impaired butterflies will fly by at random, which is mentioned as local quest in proposed algorithm.

Scent, sound, light, and temperature are all examples of modalities that can be expressed by stimuli such as those used in BOA calculations for fragrance. The entire principle of detecting and processing the modality is carried out based on three key parameters, which comprise sensory modality, stimulus strength, and power exponent. The raw input used by the receptors is referred to as sensory modality. Sensory involves calculating the energy form and processing it in appropriate manner. Modalities will now include scent, tone, colour, temperature, and, in the case of BOA, fragrance. The amplitude of the physical/actual stimuli is denoted by I, which is associated with the fitness solution in BOA. I.e. when a butterfly emits a larger amount of scent, the other butterflies in the area will detect it and become attracted to it. The exponent to which intensity is elevated is power. Normal expression, and linear response are all possible with the parameter a. Response expansion occurs as I rises and the fragrance (f) increases faster than I. As I rises, f rises more slowly than I. Response compression is the term used to describe this technique. In a linear reaction, when I increases, so does f, and vice versa. Studies on insects, mammals, and humans have found that when stimuli increase in amplitude, insects become less responsive to the changes in stimulus. As a result, in BOA, the magnitude of I is approximated using response compression.

From these ideas, the scent in BOA is expressed as a the physical force function of the stimulus, as seen in Eq. (19)

$$f = cI^a \tag{19}$$

Where, the perceived magnitude of the smell is denoted by f and the sensory modality is denoted by c, the stimulus force is denoted by I, and the modality-dependent power exponent is varied absorption degree consideration. Mostly, we will use *aandc* in the [0, 1]. The limit is the power proponent that varies with modality, and it describes absorption variance. At one end, a = 1, indicating that there is no smell absorption. As a result, achieving a single optimum is simple. If, on the other hand, a = 0, no butterfly's scent can be detected by the other butterflies. Academically, c [0,1] but functionally, the machine calculates the characteristic to be optimized. The convergence speed is impacted by the values of *a and c.*

2.4.3 Movement of Butterflies

The movements are explained as follows:
1. Total butterflies are meant to emit some kind of scent that attracts other butterflies.
2. Each butterfly will migrate at random or toward the best-smelling butterfly.
3. Butterfly stimulus amplitude is influenced or determined by the target feature's landscape.

Initialization, iteration, and completion are all steps of BOA. The initialization stage is carried out first in every BOA run, followed by iterative searching and finally by the During the iteration period, which is the second stage in the algorithm, the algorithm runs a series of iterations. Eq. (19), on the other hand, allows these butterflies to emit aroma from their habitat. During the global quest process, the butterfly moves earlier

to the fittest solution g*, which can be expressed by Eq (20) and Local search phase can be signified as in Eq. (21)

$$x_i^{t+1} = x_i^t + \left(r^2 \times g^* - x_i^t\right) \times f_i \tag{20}$$

$$x_i^{t+1} = x_i^t + \left(r^2 \times x_j^t - x_k^t\right) \times f_i \tag{21}$$

Where x_j^t and x_k^t are jth and kth solution space of the butterflies. If x_j^t and x_k^t belongs to same swarm and r is a random sum in [0, 1], then Eq. (21) converts a local random walk.

Iterations are carried out until the halting criteria are not achieved. The high number of rounds obtained is only one example of how the halting condition might be stated. The algorithm then delivers the best result with the greatest fitness at the end of the iteration procedure. The whole pseudo code is broken down into the three parts mentioned above, which are covered in "Algorithm 1."

Algorithm 1: Butterfly Optimization

$Objective function f(x), x = (x_1, x_2, \ldots, x_{dim}), dim = no. of dimensions$
$Generate initial population of n butterflies x_i = (i = 1, 2, \ldots, n)$
$Stimulus Intensity I_i at x_i is determined by f(x_i)$
$Define sensor modality c, power exponent a and switch probability p.$
$while$ $stopping criteria not met$ **do**
$for each$ $butterfly bf in population$ **do**
$Calculate fragrance for bf using Eq. (24)$
$end for$
$Find the best bf$
$for each$ $butterfly bf in population$ **do**
$Generate a random number r from [0,1]$
if $r < p$ **$then$**
$Move towards best butterfly/solution using Eq. (25)$
$else$
$Move randomly using Eq. (26)$
$end if$
$end for$
$Update the value of a$
$end while$
$Output the best solution found.$

---

3   Results and Discussion

The investigational results of the projected classification and segmentation method are presented in both quantitative and qualitative terms in this section. The proposed new scheme is assessed using two databases, BRATS 2013 and BRATS 2015. complete trial is run on an I7 Intel Core, RAM of 16.0 GB, an OS of 64-bit, and GeForce GTX 1080 NIVIDIA GPU.

3.1   Dataset Description

BRATS 2013 includes 20 (HGG/ LGG) volumes of preparation and 10 in research. BRATS 2015 has HGG as 220, volumes of LGG as 54 for training and volumes of LGG as 110 for testing process. The BRATS dataset includes three MRI views: axial, coronal, and sagittal. In the axial view, the human brain is categorized into top and bottom parts. Front and back parts of brain are obtained from the coronal view, where the right and left halves are achieved from the sagittal views.

Input slices in BRATS datasets are provided as MHA files. The MHA read header and read volume are used for extracting the brain slices of axial vision. The Matlab code is converted from the command of mat2gray and therefore, 3D slices are divided into 2D slices. The proposed ideal is trained on the axial view, because the information about upper and lower parts of brain are provided by this plane. However, when trained on coronial and sagittal views, the proposed method produces even better results. As a result, regardless of point of view, the algorithm can detect brain tumors.

Parameter	Equation
Accuracy	$\dfrac{TP+TN}{TP+TN+FP+FN}$
Sensitivity	$\dfrac{TP}{TP+FN}$
Specificity	$\dfrac{TN}{TN+FP}$
Dice Coefficient Index	$\dfrac{2TP}{2TP+FP+FN}$

Table 1: Various Parameters and its Equations

Dataset	Accuracy (%)	Specificity (%)	Sensitivity (%)	DSC	JI	FPR	FNR
BRATS 2013	92.78	88.24	96.36	0.9372	0.8818	0.1176	0.0364
BRATS 2015	98.01	95.61	99.62	0.9934	0.9868	0.0439	0.0038

Table 2: Segmentation Results

3.2 Performance Metrics

In terms of dice similarity coefficient (DSC), specificity, sensitivity, accuracy, and Jaccard Index (JI), the proposed technique efficiency is evaluated. The phrases TP, TN, FP, and FN's confusion matrix was created using several projected outcome metrics. Where,

TP – true positives

TN – true negative,

FP – false positives,

FN – false negative, and

TN – true negative

Table 1 shows the equations for the several parametric measurements employed in this research are shown.

3.3 Performance Analysis of Segmentation Technique

Table 2 depicts the performance of proposed ABC with thresholding is validated with two datasets in terms of overall performance.

Table 2 proves that in BRATS 2015 than 2013 challenge dataset the performance in terms of DSC, JSI, ACC, SP and SE. For instance, the proposed method achieved 98.01% of accuracy in BRATS 2015, where the same method achieved 92.78% of accuracy in BRATS 2013. In BRATS 2015, the DSC is 0.9934 and JSI is 0.9868, where the proposed segmentation technique achieved 0.9372 DSC and 0.8818 JSI. Table 3 displays the performance comparison of proposed ABC with thresholding with current methods for BRATS 2013.

From the above table, it is evidently proving that our proposed scheme achieved accuracy of 95.23%, where the various current methods achieved nearly 84% to 94.70%. This existing technique uses only BRATS 2013 for validation and achieved very less accuracy. But, our proposed technique uses the ABC with thresholding for accurate segmentation of brain tumor. Table 5 displays the validated results of segmentation with proposed and existing techniques for BRATS 2015 datasets.

Here, the proposed ABC with thresholding technique outperformed than current methodologies. For instance, the proposed segmentation achieved accuracy of 94%, where the other methods achieved nearly 79%

Method	Year	ACC (%)
Cordier et.al [32]	2013	84.00
Reza et.al [33]	2015	86.70
Abbasi&Tajeripour [34]	2017	93.00
UmairaNazarHussain [35]	2020	94.70
Proposed	2021	95.23

Table 3: BRATS 2013 data set Segmentation comparative results.

Method	Year	ACC (%)
Pereira et.al [36]	2016	86
Havaeiet.al [37]	2016	79
Kamnitsaset.al [38]	2017	79
Dong et.al [39]	2017	90
Proposed	2021	94

Table 4: BRATS 2015 data set Segmentation comparative results

Network Type	ACC	SEN	SPEC	F-MEASURE	FPR
Without Optimized LeNet-5 CNN	0.84	0.55	0.99	0.70	0.56
Optimized LeNet-5 CNN	0.88	0.62	0.99	0.76	0.53
Without Optimized RES Net CNN	0.87	0.65	0.99	0.78	0.50
Optimized RES Net CNN	0.93	0.75	0.995	0.85	0.49
Without Optimized Proposed Alex Net CNN	0.92	0.79	0.99	0.89	0.48
Optimized Proposed Alex Net CNN	0.98	0.96	0.9954	0.97	0.46

Table 5: Performance Analysis of proposed classifier for BRATS 2013 data set with various Network architectures

to 90% of accuracy only. While comparing with BRATS 2013 dataset, this dataset achieved low accuracy, because the images are difficult for labelling and extraction of exact tumor region. However, the this technique gained improved enhancement than various existing segmentation techniques. The next section will explain the experimental analysis of proposed classifier with and without BOA technique.

3.4 Performance Investigation of Proposed Hybrid Classification

In analyse the performance of various architectures of CNN with BOA and without BOA in terms of accuracy, specificity, FPR, sensitivity and F-measure. The various CNN architecture includes LeNet-5 [40] and RES Net [41] are compared with proposed Alex Net, which is given in Table 6 for BRATS 2013 dataset.

In this set of experiments, initially 60% for training data and remaining 40% of data is used for testing process. From this experiments, we can clearly prove that proposed Alex Net achieved better performance than other two architectures. Without BOA also, Alex Net achieved nearly 92% of accuracy, 99% of specificity and 79% of sensitivity, where RES Net achieved only 87% of accuracy, 99% of specificity and 65% of sensitivity. While implementing BOA for optimizing the learning rate of CNN architectures, the proposed Alex Net achieved 98% of accuracy and 96% of sensitivity, where RES Net achieved only 93% of accuracy and 75% of sensitivity. This proves that BOA improves the performance of various CNN architectures. The next table 7 shows the validation results of proposed architectures for BRATS 2015 datasets.

From this experiments, we can clearly prove that proposed Alex Net achieved better performance than other two architectures. Without BOA also, Alex Net achieved nearly 94% of accuracy, 99% of specificity and 89%

Network Type	ACC	SEN	SPEC	F-MEASURE	FPR
Without Optimized LeNet-5 CNN	0.78	0.46	0.99	0.63	0.62
Optimized LeNet-5 CNN	0.85	0.56	0.99	0.70	0.58
Without Optimized RES Net CNN	0.82	0.57	0.99	0.78	0.52
Optimized RES Net CNN	0.95	0.89	0.99	0.90	0.46
Without Optimized Proposed Alex Net CNN	0.94	0.89	0.99	0.90	0.46
Optimized Proposed Alex Net CNN	0.99	0.96	0.99	0.96	0.46

Table 6: Comparison of accuracy for BRATS 2015 dataset with various Network architectures

of sensitivity, where LeNet-5 achieved only 78% of accuracy, 99% of specificity and 46% of sensitivity. While implementing BOA for optimizing the learning rate of CNN architectures, the proposed Alex Net achieved 99% of accuracy and 96% of sensitivity, where RES Net achieved only 95% of accuracy and 89% of sensitivity, then LeNet-5 achieved 85% of accuracy and 56% of sensitivity. This proves that BOA improves the performance of various CNN architectures. Additionally, several sets of experiments are performed, including the accuracy test depicted in Figure 5 where 50% of training data and 50% of testing data are used. Overall accuracy of the trials using the 70:30 ratio is then shown in figure 6.

The predicted Alex Net obtained greater performance for several sets of trials, as shown by the the above data. However, even with the 50-50 split of tests, the LesNet-5 performs poorly. The following subsection concludes by comparing the suggested classifier with an already-in-use modern approach.

3.5   Comparative Analysis of Proposed Classifier

In table 7, the comparison for various existing techniques with proposed classifier is presented in terms of overall accuracy.

For BRATS 2013, the existing techniques achieved nearly 87% to 98.1% of accuracy, where the proposed classifier achieved 98.5% of accuracy. The reason is that the tumor is accurately segmented by using ABC with thresholding technique, where the existing techniques uses either Fuzzy-C Means or improved version of FCM. In set of experiments for BRATS 2015, the existing technique proposed by Sharif, M.I., et.al [44] achieved only 97.8% of accuracy, where the proposed Alex Net achieved 99% of accuracy. The reason is that learning rate of CNN architecture is optimized by using BOA technique. From these experiments, the proposed segmentation and classification technique achieved better performance for two different datasets.

4   Conclusion

Medical imaging methods are used to diagnose brain tumors which becoming more common, as brain tumors that life hacking illnesses today. A swarm of dysfunctional cells surrounds the inner part of the human brain in the tumor. It has an effect on the brain by crushing and destroying healthy tissues. It also raises intracranial
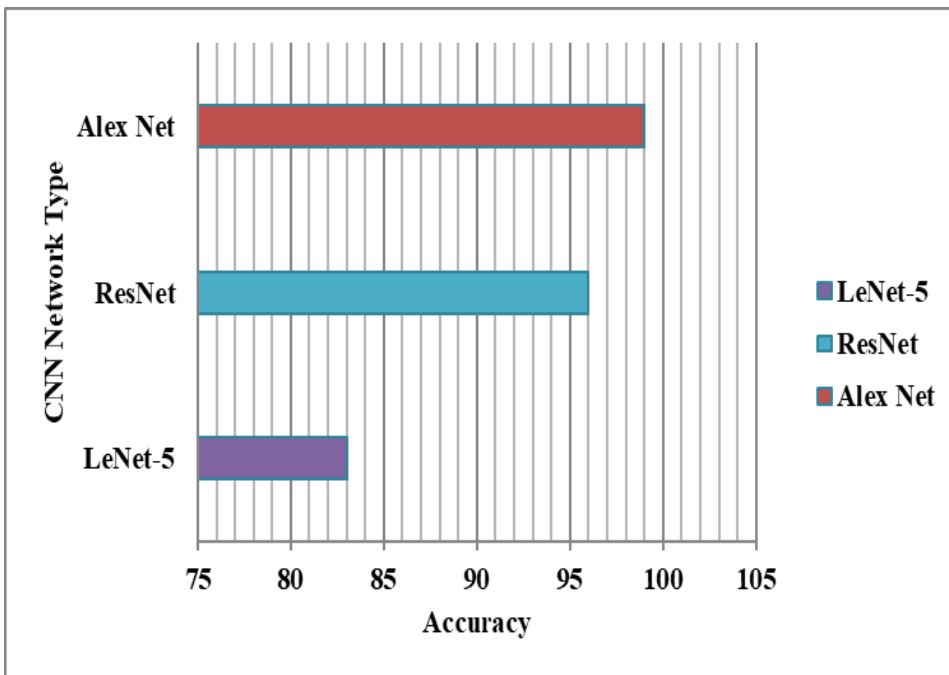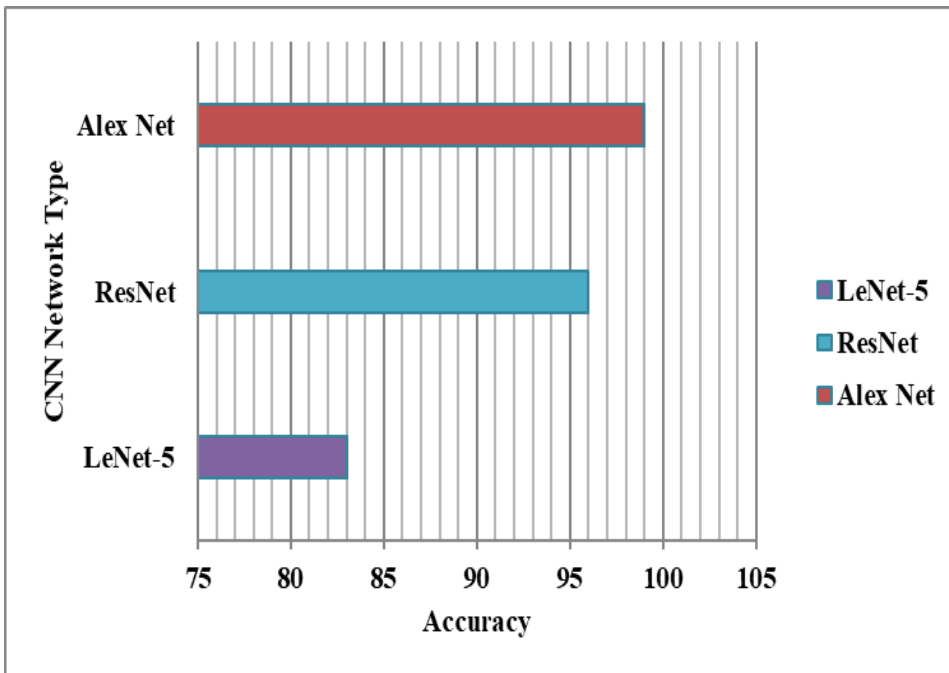
Figure 5: Comparison of Accuracy (50:50)

Figure 6: Comparison of Accuracy (70:30)

Method	Year	Dataset	ACC (%)
S. M. Reza et.al [42]	2015	BRATS 2013	86.7
M. A. Khan et.al [43]	2019	BRATS 2013	97.5
Sharif, M.I., et.al [44]	2020	BRATS 2013	98.3
Proposed Optimized CNN (Alex Net)	2021	BRATS 2013	98.5
Sharif, M.I., et.al [44]	2020	BRATS 2015	97.8
Proposed Optimized CNN (Alex Net)	2021	BRATS 2015	99

Table 7: Comparison of proposed with existing approaches accuracy

pressure, which causes tumor cell development to accelerate, potentially leading to death. Consequently, it is preferable to brain tumors detection in early stage, as this can improve the patient's chance of survival. The primary aim is to demonstrate a new strategy for tumor segmentation and detection. The suggested architecture segmented and classified benign and malignant tumor cases correctly. ABC with thresholding is used to seperate the brain tumor from the denoised images. BWT is used for extracting the features from the segmentation results. The CNN learning rate is optimized by using butterfly optimization technique for better classification. The experiments are carried out by using BRATS2013 and 2015 challenging dataset for segmentation and classification techniques validation. It is concluded, based on results that better tumor segmentation provides useful features that, in turn, have the highest precision. In the future, this study may be developed for segmenting and identifying the area of sub-tumoral parts, i.e., improve, non-enhance, and full tumor. Furthermore, to upsurge the precision and DCI of the current work, we plan to explore a more stable mechanism for a vast archive of medical images, as well as a choose classifier by integrating more than single classifier.

References

[1] Fernandes SL, Tanik UJ, Rajinikanth V, Karthik KA. A reliable framework for accurate brain image examination and treatment planning based on early diagnosis support for clinicians. Neural Computing and Applications. 2020 Oct;32(20):15897-908.

[2] Khan MA, Akram T, Sharif M, Saba T, Javed K, Lali IU, Tanik UJ, Rehman A. Construction of saliency map and hybrid set of features for efficient segmentation and classification of skin lesion. Microscopy research and technique. 2019 Jun;82(6):741-63.

[3] Sharif, M. I., Li, J. P., Khan, M. A., &Saleem, M. A. (2020). Active deep neural network features selection for segmentation and recognition of brain tumors using MRI images. Pattern Recognition Letters, 129, 181-189.

[4] Amin, J., Sharif, M., Yasmin, M., and Fernandes, S.L., A distinctive approach in brain tumor detection and classification using MRI. Pattern Recognition Letters, 2017

[5] Drozdzal, M., Chartrand, G., Vorontsov, E., Shakeri, M., Di Jorio, L., Tang, A., and Kadoury, S. (2018). Learning normalized inputs for iterative estimation in medical image segmentation. Medical image analysis, 44, 1-13

[6] Mohsen, H., El-Dahshan, E.-S. A., El-Horbaty, E.-S. M., & Salem, A.-B. M. (2018). Classification using deep learning neural networks for brain tumors. Future Computing and Informatics Journal, 3(1), 68-71.

[7] Rajinikanth, V., Satapathy, S. C., Fernandes, S. L., and Nachiappan, S., Entropy based segmentation of tumor from brain MR images-a study with teaching learning based optimization. Pattern Recogn. Lett. 94:87–95, 2017.

[8] Upadhyay, N., and AJTBjor, W., Conventional MRI evaluation of gliomas. 84 (special_issue_2):S107-S111, 2011.

[9] Nida, N., Sharif, M., Khan, M. U. G., Yasmin, M., and Fernandes, S. L., A framework for automatic colorization of medical imaging. IIOAB J. 7:202–209, 2016.

[10] Gordillo, N., Montseny, E., and Sobrevilla, P.J., State of the art survey on MRI brain tumor segmentation. 31 (7):1426–1438, 2013.

[11] Zhang, L., Song, M., Liu, X., Bu, J., and Chen, C.J.S.P., Fast multiview segment graph kernel for object classification. 93 (6):1597– 1607, 2013.

[12] Adams, R., and Bischof, L.J., ITopa, intelligence m. Seeded region growing. 16 (6):641–647, 1994.

[13] Han, J., Quan, R., Zhang, D., and Nie, F.J.I., ToIP Robust object cosegmentation using background prior. 27 (4):1639–1651, 2018.

[14] Raja, N.S.M., Fernandes, S., Dey, N., Satapathy, S.C., and Rajinikanth, V., Contrast enhanced medical MRI evaluation using Tsallis entropy and region growing segmentation. Journal of Ambient Intelligence and Humanized Computing:1–12, 2018.

[15] Rajinikanth, V., Fernandes, S.L., Bhushan, B., and Sunder, N.R., Segmentation and analysis of brain tumor using Tsallis entropy and regularised level set. Proceedings of 2nd international conference on micro-electronics, electromagnetics and telecommunications. Springer, 313–321, 2018.

[16] Deng, W., Xiao, W., Deng, H., and Liu, J., MRI brain tumor segmentation with region growing method based on the gradients and variances along and inside of the boundary curve. Biomedical engineering and informatics (BMEI), 2010 3rd international conference on, IEEE. 393–396, 2010.

[17] Zhang, L., Han, Y., Yang, Y., Song, M., Yan, S., and Tian, QJIToIP., Discovering discriminative graphlets for aerial image categories recognition. 22 12:5071–5084, 2013.

[18] Menze, B.H., Van Leemput, K., Lashkari, D., Weber, M.-A., Ayache, N., and Golland, P., A generative model for brain tumor segmentation in multi-modal images. International conference on medical image computing and computer-assisted intervention, Springer. 151–159, 2010.

[19] Akram T, Khan MA, Sharif M, Yasmin M. Skin lesion segmentation and recognition using multichannel saliency estimation and M-SVM on selected serially fused features. Journal of Ambient Intelligence and Humanized Computing. 2018 Sep 24:1-20.

[20] Ariyo, O., Zhi-guang, Q., &Tian, L. (2017). Brain MR Segmentation using a Fusion of K-Means and Spatial Fuzzy C-Means. DEStech Transactions on Computer Science and Engineering (csae).

[21] Sharif, M., Khan, M. A., Iqbal, Z., Azam, M. F., Lali, M. I. U., &Javed, M. Y. (2018). Detection and classification of citrus diseases in agriculture based on optimized weighted segmentation and feature selection. Computers and Electronics in Agriculture, 150, 220-234

[22] Brain Tumor Detection. International Arab Journal of Information Technology (IAJIT), 12(1).

[23] Pereira, S., Pinto, A., Alves, V., & Silva, C. A. (2016). Brain tumor segmentation using convolutional neural networks in MRI images. IEEE transactions on medical imaging, 35(50)1240-1251.

[24] Bahadure, N. B., Ray, A. K., &Thethi, H. P. (2018). Comparative Approach of MRI-Based Brain Tumor Segmentation and Classification Using Genetic Algorithm. Journal of digital imaging, 1-13.

[25] Sharma, M., Purohit, G., & Mukherjee, S. (2018). Information retrieves from brain MRI images for tumor detection using hybrid technique K-means and artificial neural network (KMANN) Networking communication and data knowledge engineering (pp. 145-157): Springer.

[26] Dong H, Yang G, Liu F, Mo Y, Guo Y. Automatic brain tumor detection and segmentation using u-net based fully convolutional networks. Inannual conference on medical image understanding and analysis 2017 Jul 11 (pp. 506-517). Springer, Cham.

[27] Kamnitsas K, Ferrante E, Parisot S, Ledig C, Nori AV, Criminisi A, Rueckert D, Glocker B. DeepMedic for brain tumor segmentation. InInternational workshop on Brainlesion: Glioma, multiple sclerosis, stroke and traumatic brain injuries 2016 Oct 17 (pp. 138-149). Springer, Cham.

[28] Bernal, J., Kushibar, K., Asfaw, D. S., Valverde, S., Oliver, A., Martí, R., and Lladó, X., Deep convolutional neural networks for brain image analysis on magnetic resonance imaging: A review. Artificial intelligence in medicine, 2018.

[29] Isensee F, Petersen J, Klein A, Zimmerer D, Jaeger PF, Kohl S, Wasserthal J, Koehler G, Norajitra T, Wirkert S, Maier-Hein KH. nnu-net: Self-adapting framework for u-net-based medical image segmentation. arXiv preprint arXiv:1809.10486. 2018 Sep 27.

[30] Hai J, Qiao K, Chen J, Tan H, Xu J, Zeng L, Shi D, Yan B. Fully convolutional densenet with multiscale context for automated breast tumor segmentation. Journal of healthcare engineering. 2019 Jan 14;2019.

[31] Zahari Abu Bakar, NooritawatiMd Tahir, Ihsan M Yassin, "Classification Of Parkinson's Disease Based On Multilayer Perceptrons Neural Network', Ieee Colloquium In Signal Processing And Its Applications (Cspa), 2010.

[32] Cordier, N., Menze, B., Delingette, H., &Ayache, N. (2013). Patch-based segmentation of brain tissues. Paper presented at the MICCAI challenge on multimodal brain tumor segmentation.

[33] Reza, S. M., Mays, R., &Iftekharuddin, K. M. (2015). Multi- fractal detrended texture feature for brain tumor classification. Paper presented at the Medical Imaging 2015: Computer-Aided Diagnosis.

[34] Abbasi, S., & Tajeripour, F. (2017). Detection of brain tumor in 3D MRI images using local binary patterns and histogram orientation gradient. Neurocomputing, 219, 526-535.

[35] Hussain, UmairaNazar, Muhammad Attique Khan, IkramUllhaLali, KashifJaved, Imran Ashraf, Junaid Tariq, Hashim Ali, and Ahmad Din. "A Unified design of ACO and skewness based brain tumor segmentation and classification from MRI scans." Journal of Control Engineering and Applied Informatics 22, no. 2 (2020): 43-55.

[36] Pereira, S., Pinto, A., Alves, V., Silva, C.A.: Brain Tumor Segmentation using Convolutional Neural Networks in MRI Images. IEEE Trans. Med. Imaging. 35, 1240–1251 (2016).

[37] Havaei, M., Davy, A., Warde-Farley, D., Biard, A., Courville, A., Bengio, Y., Pal, C., Jodoin, P.-M., Larochelle, H.: Brain tumor segmentation with Deep Neural Networks. Med. Image Anal. 35, 18–31 (2016).

[38] Kamnitsas, K., Ledig, C., Newcombe, V.F.J., Simpson, J.P., Kane, A.D., Menon, D.K., Rueckert, D., Glocker, B.: Efficient multi-scale 3D CNN with fully connected CRF for accurate brain lesion segmentation. Med. Image Anal. 36, 61–78 (2017).

[39] Dash, S.C.B., Mishra, S.R., Srujan Raju, K. et al. Human action recognition using a hybrid deep learning heuristic. Soft Comput 25, 13079–13092 (2021). https://doi.org/10.1007/s00500-021-06149-7

[40] Wang, T., Lu, C., Shen, G. and Hong, F., 2019. Sleep apnea detection from a single-lead ECG signal with automatic feature-extraction through a modified LeNet-5 convolutional neural network. PeerJ, 7, p.e7731.

[41] B. Padmaja, P. V. Narasimha Rao, M. Madhu Bala and E. K. Rao Patro, "A Novel Design of Autonomous Cars using IoT and Visual Features," 2018 2nd International Conference on I-SMAC (IoT in Social, Mobile, Analytics and Cloud) (I-SMAC)I-SMAC (IoT in Social, Mobile, Analytics and Cloud) (I-SMAC), 2018 2nd International Conference on, Palladam, India, 2018, pp. 18-21, doi: 10.1109/I-SMAC.2018.8653736.

[42] Kalyani, G., Janakiramaiah, B., Karuna, A. et al. Diabetic retinopathy detection and classification using capsule networks. Complex Intell. Syst. (2021). https://doi.org/10.1007/s40747-021-00318-9

[43] M. A. Khan, I. U. Lali, A. Rehman, M. Ishaq, M. Sharif, T. Saba, et al., "Brain tumor detection and classification: A framework of marker-based watershed algorithm and multilevel priority features selection," Microscopy research and technique, vol. 82, pp. 909- 922, 2019.

[44] Sharif, M.I., Li, J.P., Khan, M.A. and Saleem, M.A., 2020. Active deep neural network features selection for segmentation and recognition of brain tumors using MRI images. Pattern Recognition Letters, 129, pp.181-189.

[45] Ramu, G. A secure cloud framework to share EHRs using modified CP-ABE and the attribute bloom filter. Educ Inf Technol 23, 2213–2233 (2018). https://doi.org/10.1007/s10639-018-9713-7

[46] D. Ravi, H. Fabelo, G. M. Callico, and G. Yang, "Manifold Embedding and Semantic Segmentation for Intraoperative Guidance with Hyperspectral Brain Imaging", IEEE Transactions on Medical Imaging, Vol.36, No.9, pp.1845-1857, 2017.

[47] A. Raju, P. Ratna, Suresh, and R. Rajeswara Rao, "Bayesian HCS-based multi-SVNN: A classification approach for brain tumour segmentation and classification using Bayesian fuzzy clustering", Biocybernetics and Biomedical Engineering, Vol.38, No.3, pp.646- 660, 2018.

[48] Kalyani, G., Janakiramaiah, B., Prasad, L.V.N. et al. Efficient crowd counting model using feature pyramid network and ResNeXt. Soft Comput 25, 10497–10507 (2021). https://doi.org/10.1007/s00500-021-05993-x

[49] M. Soltaninejad, G. Yang, T. Lambrou, N. Allinson, T. L. Jones, T. R. Barrick, F. A. Howe, and X. Ye, "Automated brain tumour detection and segmentation using superpixel-based extremely randomized trees in FLAIR MRI", International Journal of Computer Assisted Radiology and Surgery, Vol. 12, No.2, pp.183-203, 2017.

C O P E

Member since 2012
JM08090

This journal is a member of, and subscribes to the principles of,
the Committee on Publication Ethics (COPE).
https://publicationethics.org/members/international-journal-computers-communications-and-control